Available online at www.garmian.edu.krd

Passer Journal of Basic and Applied Sciences

Passer 7 (Issue 1) (2025) 462-476

Original Article

Investigation of Cast in Place Pile Response to the Torsional Dynamic Load

Abdulameer Qasim Hasan *, [1], Rafi Mohammed Qasim [2], Ayad Abdulkhaleq Yahya [3]

[1] *Department of Env. and Pol. Eng., Basra Engineering College, Southern Technical University, Basra 61001, Iraq.*
[2] *Department of Fuel and Energy Eng., Basra Engineering College, Southern Technical University, Basra 61001, Iraq.*
[3] *Department of Civil Techniques, Basra Technical Institute, Southern Technical University, Basra 61001, Iraq.*

Received 28 October 2024; revised 16 January 2025;
accepted 09 February 2025; available online 22 June 2025

DOI: 10.24271/psr.2025.485990.1790

ABSTRACT

Piles foundation has been widely used to support and transfer loads to deeply strong soil. Piles have been used as foundation for tall building, tower, onshore structure, offshore structure and bridge. This paper investigates the behavior of cast in place pile under harmonic torsional loading. This study investigates the effect of pile diameter, steel tubular wall thickness, load eccentricity, torque magnitude and concrete compressive strength on the response of single pile to harmonic torsional loading. The pile response includies displacement, shear force, bending moment, torsional moment, principal stresses, skin friction, Von miss stress and soil reaction. ABAQUS Software is used to perform the numerical simulation. The pile has elastoplastic properties; similarly, the clay soil is modeled as an elastoplastic material described by the cam- clay model. The procedure used in this investigation involves fixing four parameters and varying one, such as fixing the steel tubular wall thickness, load eccentricity, torque magnitude, concrete compressive strength, and change pile diameter in order to study pile 's response. The results show that increasing the pile diameter and wall thickness leads to a decrease in the displacement by 24% , 19% respectively, while an increase in applied torque results in a 27% increase in displacement. also, It is also found that the compressive strength of concrete has a smaller effect on the response of the pile.

Keywords: deep foundation, dynamic load, pile, torsion, soil-pile-interaction.

1 Introduction

Pile foundation are a type of deep foundation; capable of transferring structural loads to deeper, more competent soil layers through end bearing and skin friction along the pile-soil interface. Pile foundations are widely used in both onshore and offshore structures, including tall buildings, bridges, infrastructure, and urban overpasses. Due to the eccentricity in applied horizontal loads, significant torsional moments will grow and develop, this challenge must be addressed in pile foundation design. Therefore, understanding the torsion-pile-soil interaction is essential to avoid substructure failure, which could directly compromise in integrity of the superstructure. Several researchers have investigated the behavior of piles under torsional and combined loading condition. Some of the relevant studies in this field are highlighted below. A method was proposed to estimate the torque capacity of piles subjected to vertical forces, incorporating the effects of expansive force effects, ground heave after immersion, function of load transfer at soil-pile interface with negative and positive friction resistance. Finite difference method was employed to obtain a nonlinear solution for the behavior of single pile under vertical loading [1]. A numerical analysis conducted by using finite element method to model the torsion-pile-soil interaction. ANSYS software was utilized to perform the required simulation. The above studies deal with torsion magnitude, load eccentricity, pile length and pile diameter on the soil domain size. The soil has been modelled by Drucker-Prager. Based on the results, it was found the load eccentricity, torsion magnitude and pile diameter had a significant influence on the behavior of single pile, while a relatively minor effect was observed for pile length [2]. An analytical solution was employed to study the dynamic behavior of a pipe pile subjected harmonic torque in unsaturated soils. Relying on porous media three-phase wave equations, the inertial coupling influence between gas and water, also capillary pressure and saturation degree effect on the dynamic shear modulus of soil, were considered. Elastic theory has been used to model pile in one-dimension. The suggested analytical solution has been verified by being compared with two other solutions [3].

* Corresponding author
E-mail address a.almubarak@stu.edu.iq (Instructor).
Peer-reviewed under the responsibility of the University of Garmian.

A new method was proposed to investigate the response of an end-bearing pile that is embedded in an isotropic and homogeneous soil layer under harmonic torque loads applied at the head of pile. In this method, the soil has been assumed to be linear viscoelastic. Vertical and radial displacements are ignored. The variational approach and Hamilton's principles were adopted to solve analytically the equations of pile-soil displacement by adopting an iterative algorithm [4].
The characteristics of bearing investigated by for a single pile subjected to combined loading (vertical loads and torque) at the pile head. The governing equations of pile shaft displacement have been suggested in the consideration of load transfer method. A new numerical model analysis was proposed to modify the vertical and circumferential ultimate friction resistance of the pile side. MATLAB program was employed to obtain the nonlinear solution for a single pile under combined loading conditions with various loading paths. In addition, the bearing capacity envelopes were plotted by [5]. An exact solution developed in order to investigate harmonic torsional vibration with time for pile with elastic properties embedded a radially inhomogeneous saturated soil [6].
The wedged soil model relied to derive an analytical solution for a stepped pile subjected to torsional dynamic load. A parametric study was also performed to investigate the effect of geometrical parameters and boundary of the wedged soil on the torsional impedance of the stepped pile [7]. A numerical study was conducted to examine the behavior of offshore platform under torsional loading. The soil in above model was modelled as both elastic and elastoplastic with various domains size being considered. The results were focused on the influence of torsional loading on pile head displacement, rotation, shear force, bending moment and shear stress [8].
The performance of pile was subjected to cyclic torsional loading was studied. The analysis was carried out using the boundary element method. The numerical model was verified by being compared with available experimental data. The model is used to carry out a parametric study to realize the effect of cyclic torsional load parameters on the pile axial capacity. From the parametric analysis, it was conducted that the amplitude, frequency and number of cycles have a significant influence on the pile's cyclic torsional response [9].
The behavior of an end-bearing single pile subjected to dynamic torsional loading was investigated. The pile was embedded in radially inhomogeneous saturated soil. Soil was modeled using Biot's two-phase linear theory [10].
An analytic solution was developed in order to investigate the dynamic response of a large diameter, end-bearing pipe pile subjected to dynamic torsional loading in saturated viscoelastic soil. One dimensional elastic theory and Biot's two phase linear theory were adopted to simulate wave propagation in pile and saturated soil. The equations of dynamic equilibrium for the pile, inner soil and outer soil were established. The obtained results were compared with those of a solid pile in elastic saturated soil to verify the validity of the solution [11]. An analytic solution was developed for the response of single pile subjected to torsional load [12].
The dynamic response of an end-bearing pile embedded in saturated isotropic soil and subjected to a harrmonic torsional load was examined. A parametric study was performed to investigate the effect of anisotropy on the pile's torsional vibration characteristics [13].
An analytic solution was proposed in order to study the behavior of a pile to torsion vibration. The pile is embedded in poroelastic homogeneous medium and torsional harmonic loading is applied. The numerical selected results were found to analysis the effect of the important variables on the torsional impedance at pile head level [14]. The pile dynamic response under transient torsion load was studied. The pile was embedded in transversely saturated isotropic soil. The soil-pile system was divided in thin layers, and the governing equations of pile segment and soil layer were solved by Laplace transform [15]. The pile's dynamic response under harmonic torsional loading was analyzed. The pile was embedded in saturated half space. Numerical results focused on the effects of pile flexibility, geometric properties of the saturated soil-pile system, excitation frequency on the pile torque, coupled impedance and torsional angle [16]. The response of elastic cylindrical pile which was embedded in poroelastic homogeneous soil medium and the pile is under torsional load was studied [17]. The torsional vibration of an elastic foundation placed on a poroelastic saturated medium was investigated [18]. An analytical solution was adopted to studyze the elastic pile subjected to axial loadings and transient torsion [19]. An end-bearing pile under torsional vibration and embedded in a viscoelastic soil medium was examined [20].
This paper is aimed to investigate the effect of variation in pile diameter, steel tubular wall thickness, concrete compressive strength, eccentricity above ground level, and torsional harmonic load magnitude on the overall behavior of torsion-pile-soil interaction. Therefore, the main objective of this paper is to study the behavior of single piles subjected to torsional loading, by analyzing the variation in displacement, shear force, bending moment, torsion, surface friction, soil reaction, principal stress, and von Mises stress along the pile length.

2 Materials and numerical simulation

The current paper is concerned with torsion-pile-soil interference of cast in place pile under torsional harmonic vibration loading. In this study, the single pile was embedded in clay soil. The materials and numerical simulation are explained briefly as below

2. 1 Materials

The pile is composed of two parts: the outer part is referred to as steel tubular pipe and the inner part is referred to concrete which is cast in place [21]. Table (1) and table (2) presents the physical properties of concrete and steel materials respectively [22]. The concrete material is represented by damage plasticity model, while the steel is modeled by elastic model. In this study, an elasto-plastic material model was adopted for the single cast in place pile under different magnitude of harmonic torsional load [23, 24].

Table 1: Concrete material characteristic.

Variable	Unit	Value
Mass Density	Kg/m^3	2380
Dilation Angle	Degree	40
Young's Modulus	MPa	23450
Eccentricity		0.1
Fbo/fco		1.16
K		0.667
Poisson's ratio		0.18

Table 2: Steel material characteristics.

Variable	Unit	Value
Mass Density	kg/m3	7850
Young's Modulus	MPa	2E9
Poisson's ratio		0.3

Various values for steel tubular pipe wall thickness were used in the numerical simulation, these thickness values included 5mm, 10mm, 15mm, and 20mm. Also, various values of compressive strength of the concrete material were also adopted in the simulation, and these values were 25MPa, 30MPa, 35MPa, and 40MPa. In addition, different pile diameters were used in the simulation, specifically 500mm, 800mm, 1000mm, and 1500mm. Furthermore, various values of pile eccentricity were considered, including 0 m (no load eccentricity), 0.4m, 0.7m, and 1m. The pile head was assumed to be free to move and rotate. The pile length, or the pile embedded depth was equal to 30 m. The dry soft clay soil was described as an elastoplastic material and was modeled by cam-clay model. The soil characteristics are given in Table (3) [25].

Table 3: Soil characteristics.

Variable	Unit	Value
Mass Density	Kg/m^3	1700
Young's Modulus	MPa	8.6
Poisson's ratio		0.4
Cohesion	KPa	20
Void ratio		0.74
M		1.1
λ		0.26
k		0.02
β		1

For boundary conditions, the boundaries were measured from the center of the pile. The distance from the pile center to the sides of the soil domain size was set to 8D, and the distance from the pile end to the bottom of the soil domain size was also set to 8D, where D represents the pile diameter [26, 27]. For the soil boundary conditions at the sides of the soil domain, in y-direction the points or nodes were allowed to move only in the x-direction, while in the x-direction, the points or nodes were allowed to move only in the y-direction. Moreover full fixed boundary conditions were applied at the bottom of the soil domain size. The boundary condition at pile end was considered free to move and rotate. Interface element (interface penalty) were utilized between pile and the surrounding clay soil. Surface to surface interface was employed to model the required linkage between pile surface and surface of the surrounding soil. Tangential behavior was defined to describe the contact properties, with a friction coefficient equal to 0.36.

The full bound case was utilized to model the contact between inner surface of the steel tubular member and pile concrete surface. This means that any nodes along the pile depth must be coincided directly with the neighboring nodes on the steel tubular member. The applied load is described as a harmonic torsional load with different values of the applied torque. The values of torque considered in this investigation were 250 kN.m, 500 kN.m, 1000 kN.m, and 2000 kN.m. The harmonic torsional vibration load is defined according to the following equation:

$$F = T \ \sin t \tag{1}$$

Where F: applied load, T: applied torque, t: time of the applied torque, in this study the time of the applied torque equal to 20 second.

2. 2 Numerical simulation

ABAQUS Software 2020 was utilized to perform the required simulation of a single pile under harmonic torsional vibration, considering clay soil as an elasto-plastic material. The input data to the software consisted of the geometrical dimensions of the pile and soil domain size, along with the boundary conditions of the whole system. The input harmonic load was applied such as force function of torque and time. The solution was obtained using a dynamic loading model to simulate the vibration response of the single pile to harmonic torsional loading. Brick element C3D20R: a three dimensional element with 20 nodes was used to model both the soil and the pile for the current problem [28]. The linear and nonlinear material characteristics of the soil and pile, respectively, were assigned to the brick elements to provide a complete representation of the material properties. Figures (1) shows the whole pile-clay soil system. The total number of elements adopted to model the soil was 155000, while 1984 element were used for the concrete pile, 976 elements were assigned to the steel tubular member.

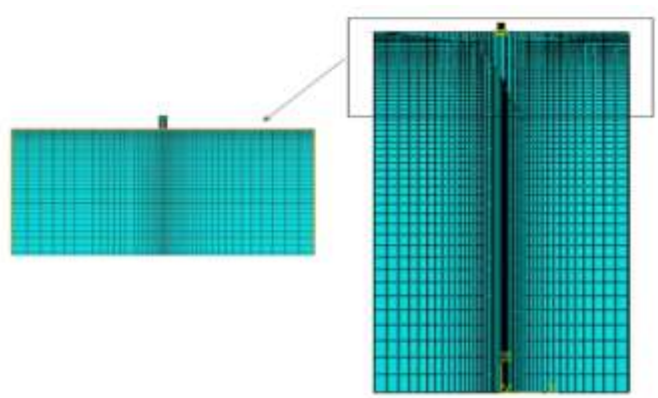

Figure 1: Pile – clay soil system mesh.

3 Results and Discussions

3. 1 Pile displacement

The pile displacement profile is considered as a reflection of the behavior of a single pile under the applied load and the surrounding soil conditions. Moreover, several noticeable parameters were founf to affect the pile behavior. Therefore, these parameters, such as pile diameter, steel tubular wall thickness, load eccentricity, torque magnitude, and concrete compressive strength. The procedure adopted to evaluate the pile response was represented by fixing four parameters and varying the remaining one, after which the displacement profile was plotted. Figures (2-a) demonstrates the pile displacement profile along the total pile depth while the pile diameter was varied, and the steel tubular thickness, load eccentricity, torque magnitude, and concrete compressive strength. It is evident from the figures that as the pile diameter increased, the pile displacement decreased sharply due to the rise in the pile moment of inertia, which is influenced by pile diameter. This was reflected in the pile deformation. The maximum pile head displacement was observed when D=500mm, while the minimum pile head displacement occured at D=1500mm. it is implied from the figures for all pile diameters, the displacement equal to zero after embedded depth equal to 10m. Additionally, the displacement profiles were identical for all pile diameters. Figures (2-b) demonstrates the pile displacement profile with variation in steel tubular wall thickness, while pile diameter, load eccentricity, torque magnitude, and concrete compressive strength were kept constant. As the wall thickness increased, the pile displacement dropped sharply due to the increase in moment of inertia of steel tubular member, which depends on wall thickness. This was reflected in the pile deformation. The maximum pile head displacement was observed at t=5mm, while the minimum pile head displacement occured at t=20mm, it is implied from the figures, for cast in place piles with different steel tubular wall thickness, the displacement became zero after embedded depth equal to 10m. Furtherfore, the displacement profiles were nearly regardless of wall thickness. Figures (2-c) demonstrate the pile displacement profile along the total pile depth with changing the load eccentricity and fixing pile diameter, steel tubular thickness, torque magnitude, and concrete compressive strength. It is evident from figures with increases that occur in pile load eccentricity, the pile displacement rose dramatically due to the decrease in the pile's resistance to the applied load. Consequently, more load was transferred to the surrounding soil, leading to this response. The maximum pile head displacement was observed when e=1 m, while the minimum pile head displacement was recorded when there was no load eccentricity. It is implied from figures for all pile load eccentricity, the displacement became zero after an embedded depth of 10 m. Additionally, the displacement profile was found to be identical for all values of pile load eccentricity. Figures (2-d) demonstrate the pile displacement profile along the total pile depth with the torque magnitude being varied, while the pile diameter, steel tubular thickness, load eccentricity, and concrete compressive strength were kept constant. It is evident from the figures that, with an increases in the applied torque, the pile displacement increased significantly, owing to the increase in load transferred to the pile in spite of pile resistance to the applied torque. The maximum pile head displacement was observed when T=2000 kN.m, while the minimum pile head displacement was recorded when T= 250 kN.m, it is implied from the figures that, for all applied torque magnitude, the displacement was equal to zero after an embedded depth of 10m. Also, the displacement profile was found to be identical for all applied torque loads. Figures (2-e) demonstrate the pile displacement profile along the total pile depth with changing concrete compressive strength, while pile diameter, steel tubular thickness, load eccentricity, and torque magnitude were kept constant. It is evident from figures that with an increase in concrete compressive strength, the pile displacement was observed to rise gradually. Moreover, the maximum displacement was consistently recorded at the pile head, despite adopting various values for concrete compressive strength. The displacement was founf to be equal zero after an embedded depth of 10 m. Also, the displacement profile appearded identical regardless of the variation in concrete compressive strength values. This was attributed to the fact that changes in the concrete modulus of elasticity and pile's cross sectional moment of inertia were considered very small.

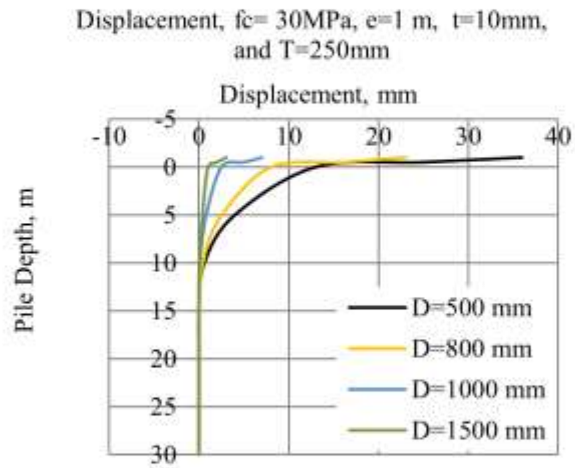

Figure 2. a: Pile displacement when change pile diameter.

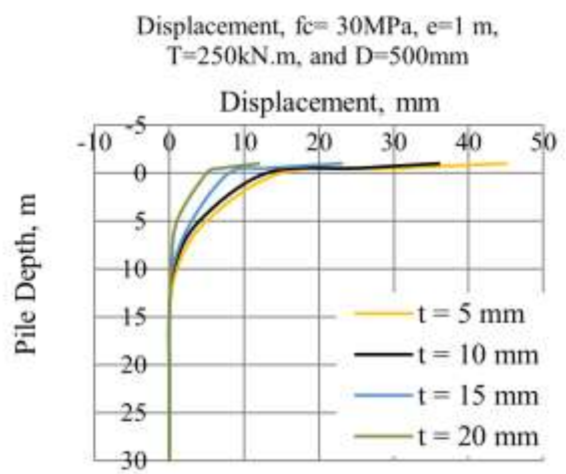

Figure 2. b: Pile displacement when change pile thickness.

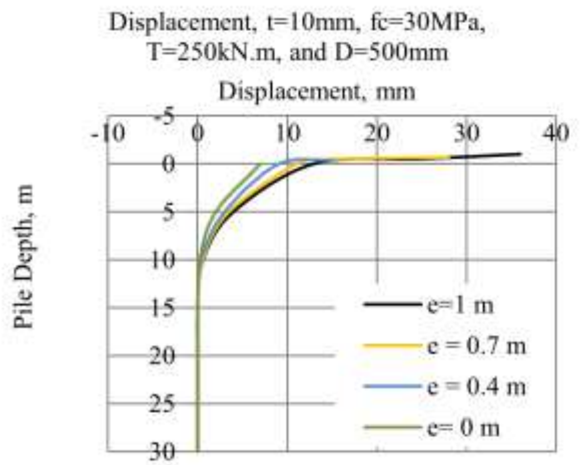

Figure 2. c: Pile displacement when change load eccentricity.

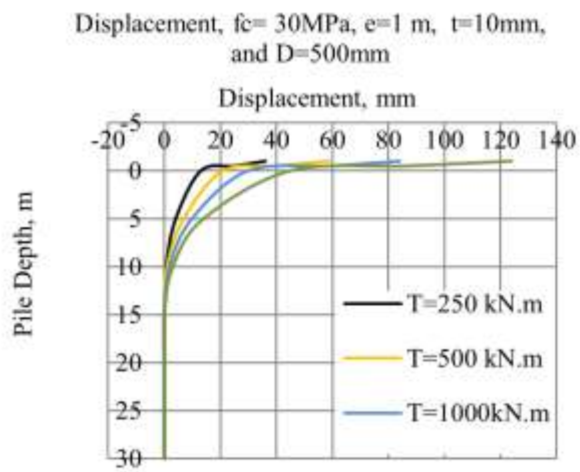

Figure 2. d: Pile displacement when change torsion load.

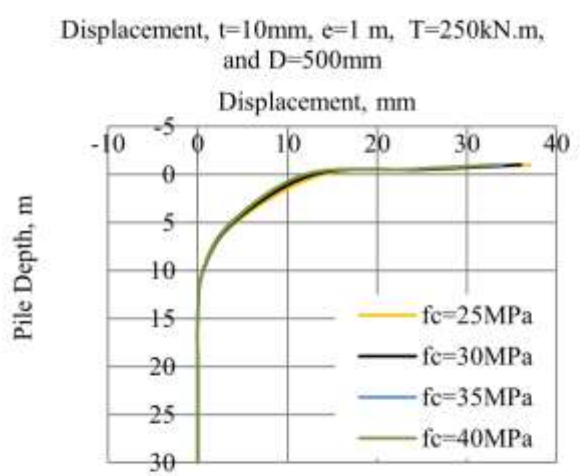

Figure 2. e: Pile displacement when change concrete compressive strength.

3. 2 Shear force

The same procedure as described in the previous section that dealt with pile displacement, was also adopted in this study to investigate the pile shear force response. Figures (3-a) show the variation of pile shear force with depth, based on different pile diameter. The shear force profile was found to be similar regardless of the variation in pile diameter. Maximum shear force values were obtained for a pile diameter equal to 500 mm, while the minimum shear force values were observed for a pile diameter equal to 1500 mm. The remaining diameters produced moderate shear force values that lay between the maximum and minimum values, respectively. Positive shear force values were observed from the ground surface to a depth of 8 m, after which an inflection point occured, and the shear force changed to negative values. Beyond of depth of 16 m, the shear force became constant and reached zero value. The fluctuation in the shear force values was found to depend on both pile stiffness and soil stiffness.

Figures (3-b) show the variation of pile shear force with depth, based on different steel tubular wall thickness. The shear force profile was found to be similar regardless of the variation in wall thickness. Maximum shear force values were obtained with wall thickness equal to 5 mm, while minimum shear force values were obtained with wall thickness equal to 20 mm. The remaining cases exhibited moderate values for shear force, which lay between the maximum and minimum values respectively. Positive shear force values were observed from the ground surface to 8 m below ground, after which an inflection point occurred, and the shear force changed to negative values. Beyond a depth of 16 m, the shear force became constant and reached zero. The fluctuation in the shear force values was attributed to steel tubular wall stiffness and soil stiffness. Figures (3-c) show the variation of pile shear force with depth, based on different load eccentricities. The shear force profile was also found similar regardless of the variation in eccentricity of load. Maximum shear force values were obtained in the case of no load eccentricity, while minimum values were observed with a load eccentricity equal to 1m. The remaining values lay between the maximum and minimum shear forces values. Positive shear force values extended from the ground surface to 8m depth, followed by an inflection point, where the shear force changed to negative values. After that, from depth equal to 16m the shear force became constant and equaled zero value. The fluctuation in the shear force values depended on the load transfer from soil to the pile, and the interaction between transfer waves and reflect waves by the soil domain size. Figures (3-d) show the variation of pile shear force with depth, depending on the applied torque. The shear force profile was observed to be similar similar regardless the variation in torque magnitude. Maximum shear force values were obtained when torque equaled 2000 kN.m, while the minimum shear force values were found at 250 kN.m. intermediate torque magnitudes resulted in moderate shear force values lying between the maximum and minimum values respectively. Positive shear force values persisted from the ground surface to a depth of 8 m, after which an inflection point occurred, changing the shear force to negative values. After that, from depth equal to 16m, the shear force became constant and has zero value.

The fluctuation in the shear force values was founf to rely on the magnitude of the applied load, the load transfer from soil to the pile, and the interaction between transfer waves and reflect waves within the soil domain size. Figures (3-e) show the variation of pile shear force with depth, based on different concrete compressive strength of pile. The shear force profile was observed to be similar regardless of the variation in compressive strength. Maximum shear force occurred at pile head, regardless of the values of concrete compressive strength. Positive shear force values were observed from ground till 8m below ground, after which an inflection point was observed, and the shear force changed to the negative values. After that, from depth equal to 16m the shear force become constant and has zero value. There was no noticeable variation in the obtained result, and this is reflected in the Figures. This occurred due to the small variation in concrete modulus of elasticity, which was based on compressive strength.

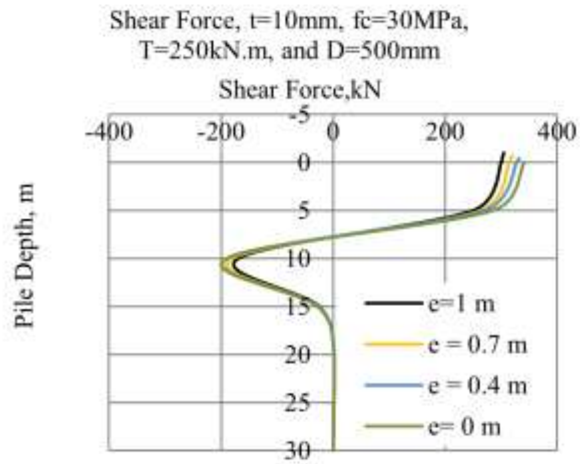

Figure 3. c: Shear force along pile when change load eccentricity.

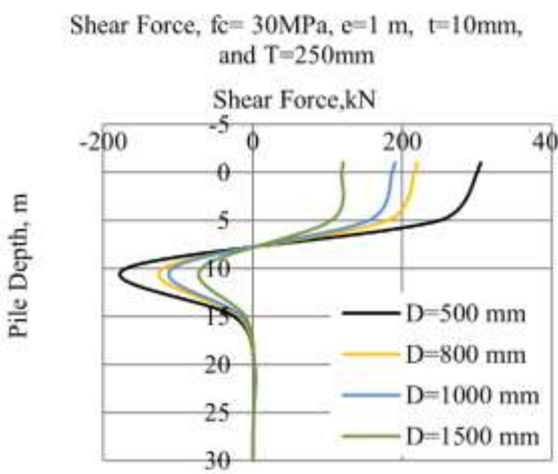

Figure 3. a: Shear force along pile when change pile diameter.

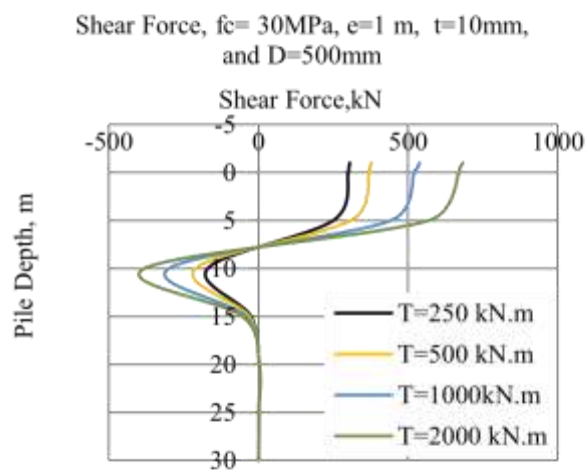

Figure 3. d: Shear force along pile when change torsion load.

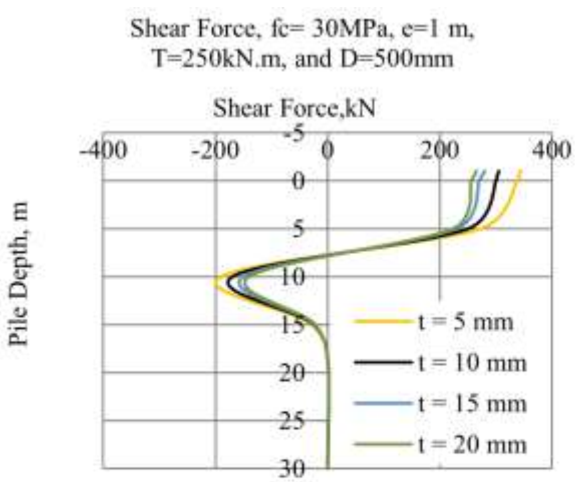

Figure 3. b: Shear force along pile when change pile thickness.

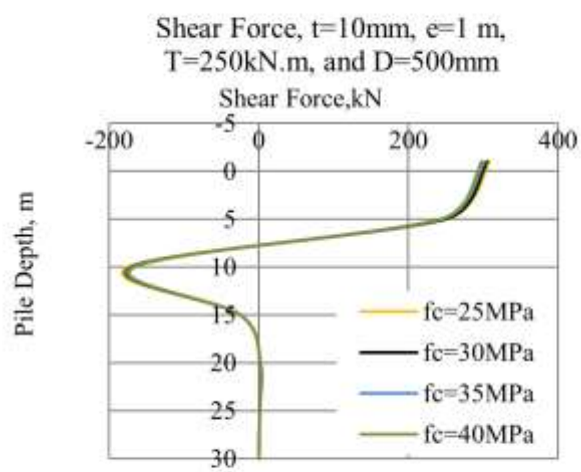

Figure 3. e: Shear force along pile when change concrete compressive strength.

3. 3 Bending moment

The same procedure, which was described in the previous section dealing with pile displacement, was also adopted in this study to investigate the pile bending moment response. Figures (4-a), (4-b), (4-c), (4-d) and (4-e) illustrate the noticeable variation in bending moment along the pile depth, considering pile diameter, steel tubular wall thickness, load eccentricity, torque magnitude, and concrete compressive strength. For Figures (4-a) the maximum bending moment was observed at D=500mm, while the minimum bending moment occured at D=1500mm. The variation in the result was attributed to the higher stiffnessof piles with greater diameters as compared to those with smaller diameter. Additionally, the fluctuation in the result was influenced by soil stiffness. For Figures (4-b), the maximum bending moment occured at t=5mm, while the minimum bending moment was recorded at t=20mm. The variation in the results was due to the increased steel wall stiffness with increasing wall thickness. For Figures (4-c), the maximum bending moment was obtained in the case where there was no load eccentricity, while the minimum bending moment occured at e=1m. The variation in the results was attributed to the drop in pile resistance to the applied load. For Figures (4-d), the maximum bending moment was recorded at T=2000 kN.m, while the minimum bending moment occurred at T=250 kN.m. The variation in result occurred from the change in the magnitude of the applied torque at the pile head. For Figures (4-e), the maximum bending moment was observed at the pile head for all values of concrete compressive strength. For all Figures from (4-a) to (4-d), the bending moment profile was found to be similar regardless of the variation in parameters. The bending moment profile began with positive values at the ground surface and extended until it changed to negative values at a depth 13m. This position indicated an inflection point where the bending moment changed from positive to the negative. Between depths of 21m and 23m, the bending moment became constant with depth.

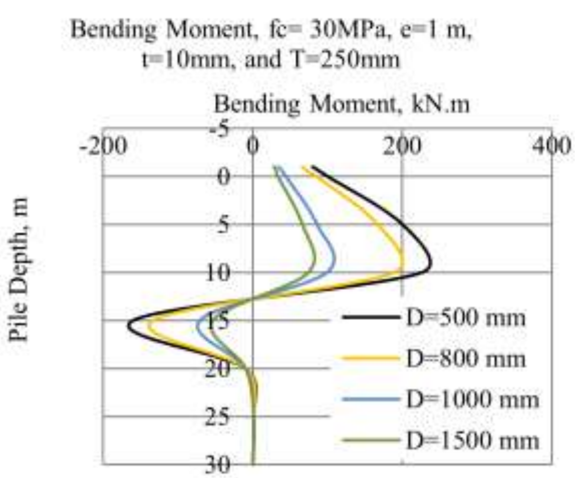

Figure 4. a: Bending moment along pile when change pile diameter.

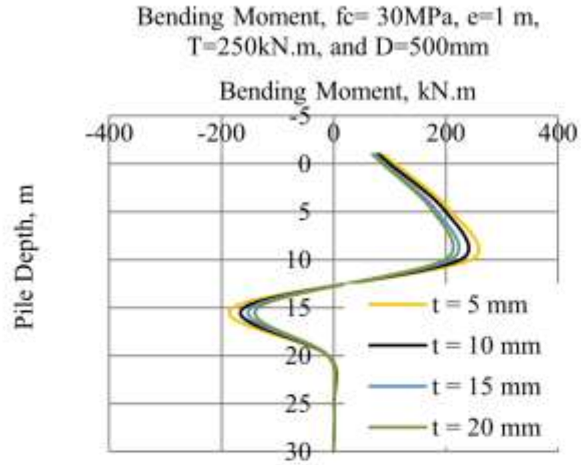

Figure 4. b: Bending moment along pile when change pile thickness.

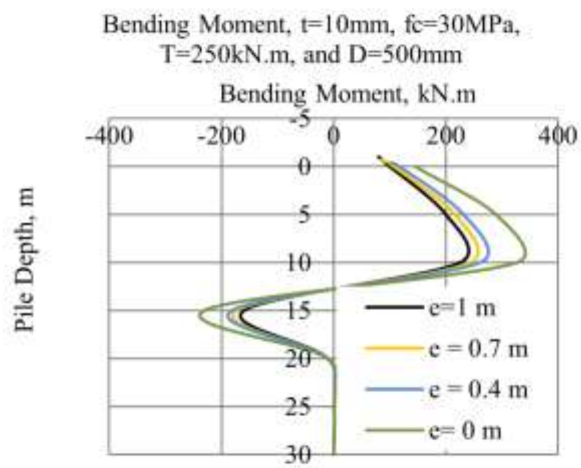

Figure 4. c: Bending moment along pile when change load eccentricity.

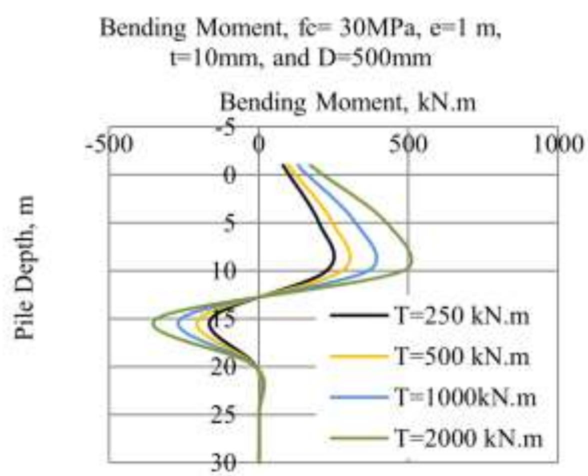

Figure 4. d: Bending moment along pile when change torsion load

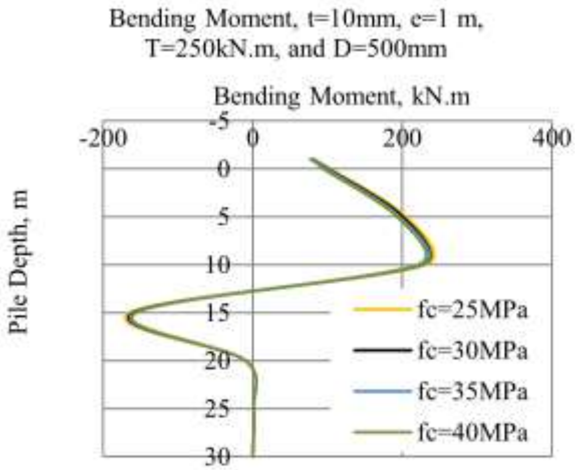

Figure 4. e: Bending moment along pile when change concrete compressive strength.

3. 4 Torsion

The same procedure which was described in the previous section dealing with pile displacement, was also adopted in this study to investigate the pile torsional response. Figuress (5-a), (5-b), (5-c), (5-d) and (5-e) illustrate the noticeable variation in torsion along the pile depth, considering pile diameter, steel tubular wall thickness, load eccentricity, torque magnitude, and concrete compressive strength. Based on Figure (5-a), the maximum torsion was observed at the pile head. Maximum values of torsion were found at D=500mm, while the minimum values of torsion were found at D=1500mm. Similarly, Figure (5-d) shows that the maximum torsion occurred at pile head. Maximum values of torsion were found at T=2000 kN.m, while the minimum values of torsion were found at T=250 kN.m. For both figurers, the magnitude of torsion transferred through pile was directly reflected in the response of the pile to the applied torsion with depth.

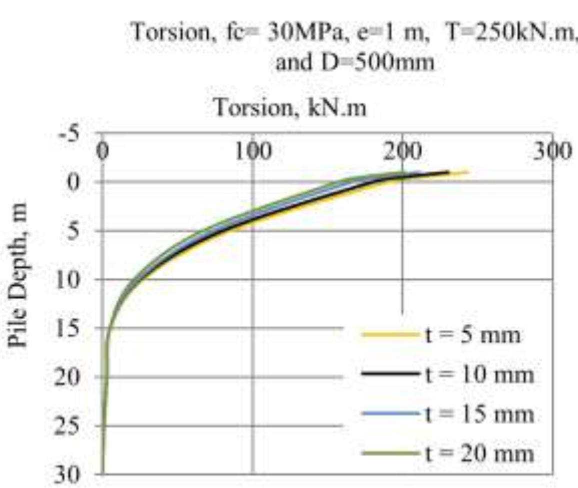

Figure 5. a: Torsion along pile when change pile diameter.

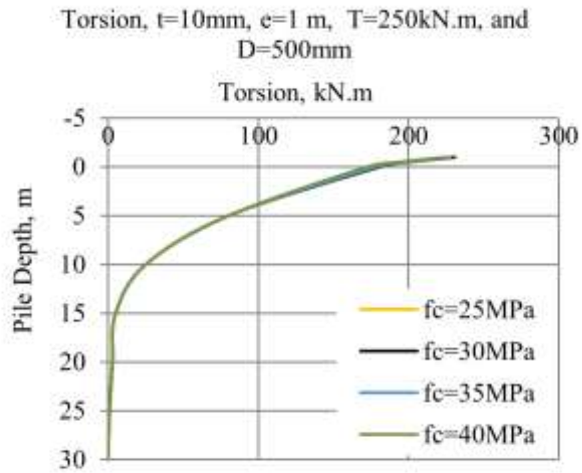

Figure 5. b: Torsion along pile when change pile thickness.

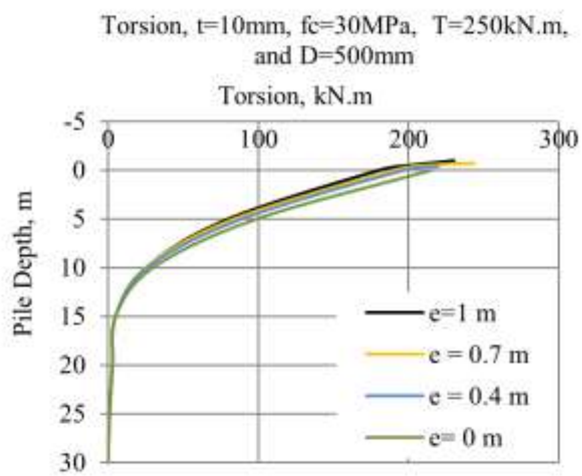

Figure 5. c: Torsion along pile when change load eccentricity.

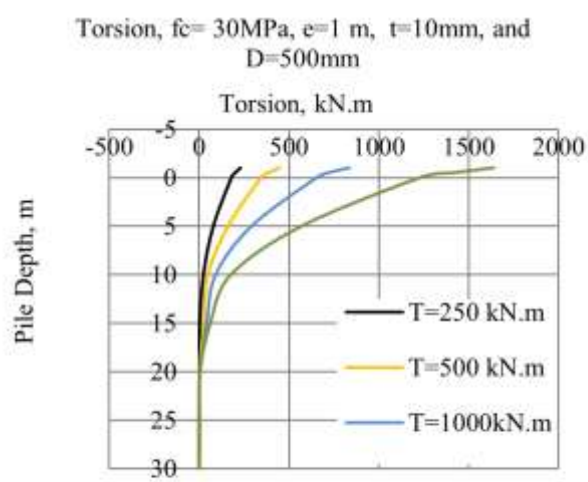

Figure 5. d: Torsion along pile when change torsion load.

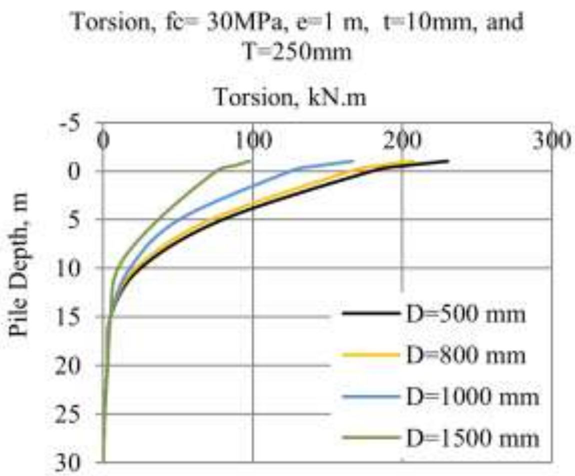

Figure 5. e: Torsion along pile when change concrete compressive strength.

In addition, the pile cross sectional resistance to the applied torsion contributed directly on the pile's response under torsional load. Figurers (5-b), (5-c) and (5-e) show similar behavior of the pile under torsional load, where the maximum torsion occured at the pile head. The variation in the results of Figurer (5-b) and (5-c) depend mainly on the values of the applied torsion and the resistance of Figure (5-b) and (5-c) depended primarily on the values of the applied torsion and the pile's resistance to load transfer. For Figure (5-e), the variation in compressive strength was found a minor effect on the response of pile to the torsional load. The torsion magnitude became constant beyond a depth 20m, regardless of variation in the previous parameters.

3. 5 Skin friction

The same procedure which was described in the previous section dealing with pile displacement, was also adopted to evaluate skin friction along the pile depth. Figures (6-a), (6-b), (6-c), (6-d) and (6-e) illustrate the noticeable variation in skin friction along the pile depth, considering pile diameter, steel tubular wall thickness, load eccentricity, torque magnitude, and concrete compressive strength. Figure (6-a) illustrates the alteration in the skin friction with depth for various pile diameter. It is evident from figure that as the pile diameter increase, the skin friction decreases, owing to the ifact that an increase in diameter leads to an increase in pile's circumference. Therefore, this causes a rise in pile's resistance to the applied load through skin friction, which is developed between the pile circumference and the surrounding clay soil.

Figures (6-b) illustrates the alteration in skin friction with depth for various steel tubular thickness. For Figure (6-b), the maximum skin friction was observed at t=20mm, while the minimum skin friction was occurred at t=5mm. The variation in results occurred due to the increase in the surrounding area of the pile, which provided larger resistance. Figures (6-d) illustrates the alteration in the skin friction with depth for various values of applied torque. For Figure (6-b), the maximum skin friction was observed at T=250 kN.m, while the minimum skin friction was occurred at T=2000 kN.m. The variation in results was attributed to the increase in pile thickness, which resulted in larger stiffness and largeer moment of inertia to resist the applied torque. Figures (6-c) and (6-e) illustrate the alteration in the skin friction with depth for various values of load eccentricity and compressive strength. The maximum value of skin friction occurred at the pile head, regardless various values of load eccentricity and compressive strength. It can be inferred that both load eccentricity and concrete compressive strength had a minor effect on skin friction values. In general, for all figures, the skin friction curves exhibited an inflection point at depth equal to 10 m. In this study, the skin friction changed from a negative value to positive value.

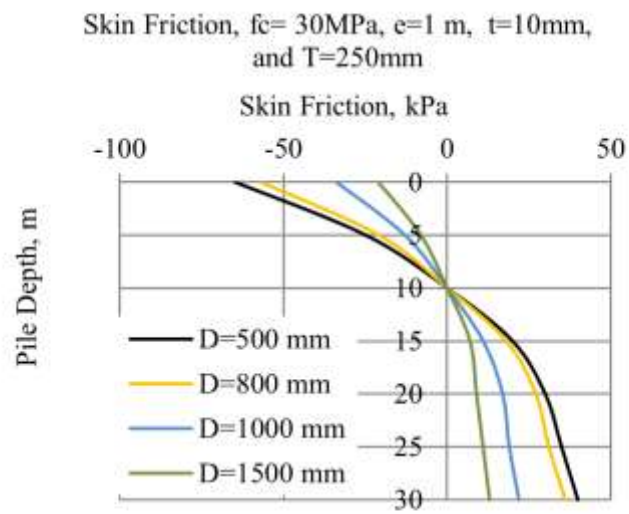

Figure 6. a: Skin friction along pile when change pile diameter.

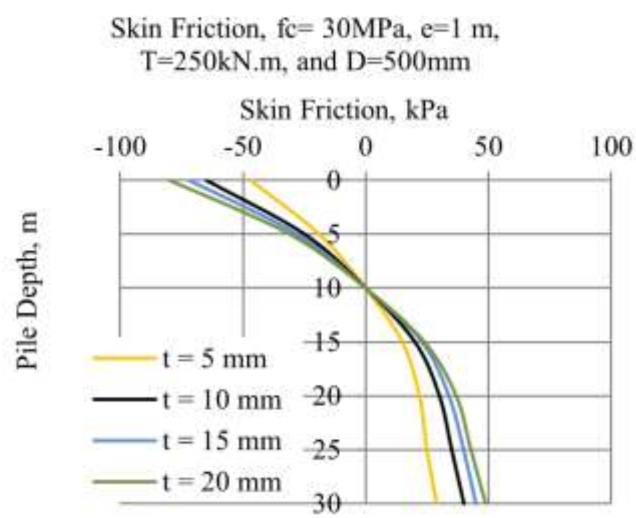

Figure 6. b: Skin friction along pile when change pile thickness.

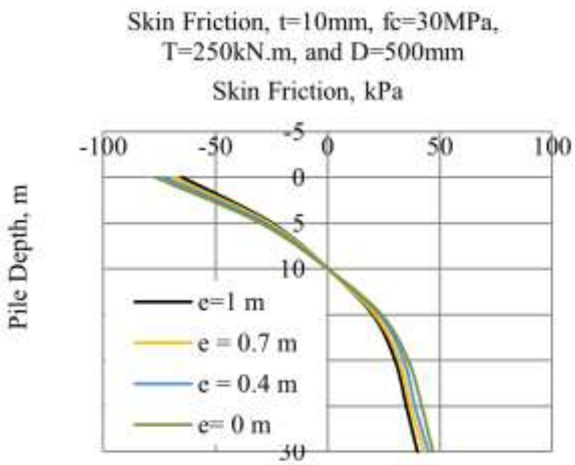

Figure 6. c: Skin friction along pile when change load eccentricity.

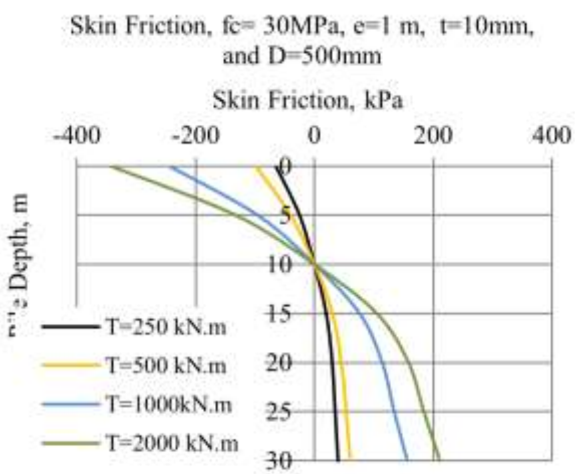

Figure 6. d: Skin friction along pile when change torsion load.

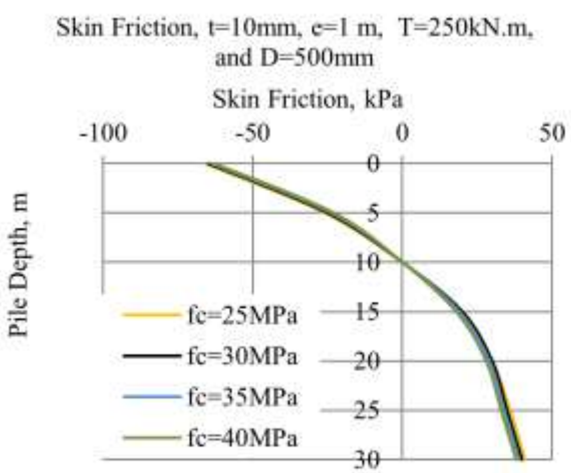

Figure 6. e: Skin friction along pile when change concrete compressive strength.

3. 6 Principal stresses

The same procedure which was described in the previous section dealing with pile displacement, was also adopted in this study to evaluate pile principal stresses. Figures (7-a), (7-b), (7-c), (7-d) and (7-e) illustrate the noticeable variation in principal stresses along the pile depth, considering pile diameter, steel tubular wall thickness, load eccentricity, torque magnitude, and concrete compressive strength. Based on all figures, it is evident that the maximum values of principal stresses occurred when the parameter had the lowest value, while the minimum values of principal stresses occurred when the parameter had the greatest value. Many variable were found to influence the variation of principal stresses value, such as pile cross- section, pile moment of inertia, pile resistance to applied load, pile stiffness, load transfer to soil, and soil resistance. Figures (7-a), (7-b), (7-c), (7-d) and (7-e) showed identical behavior regardless the variation in parameters.

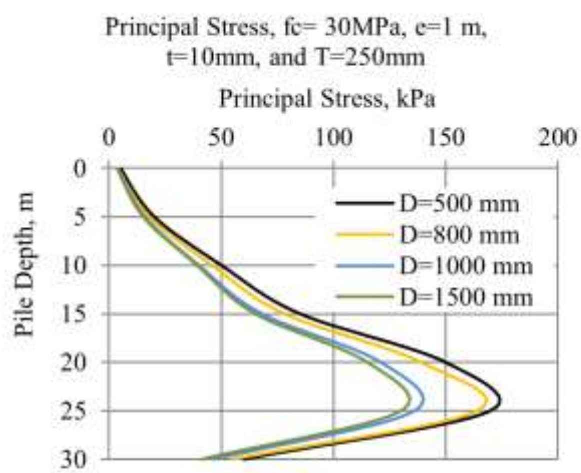

Figure 7. a: Principal stress along pile when change pile diameter.

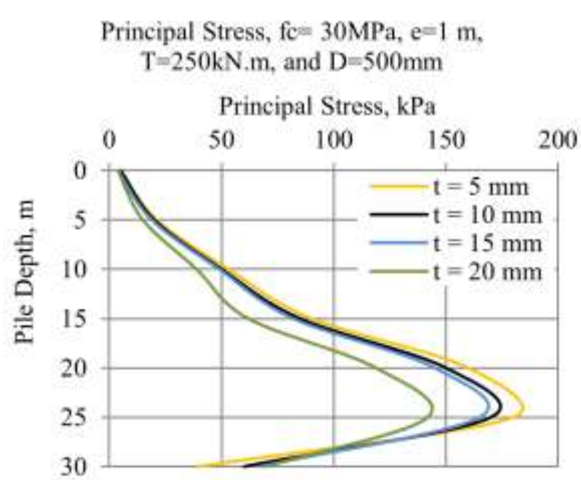

Figure 7. b: Principal stress along pile when change pile thickness.

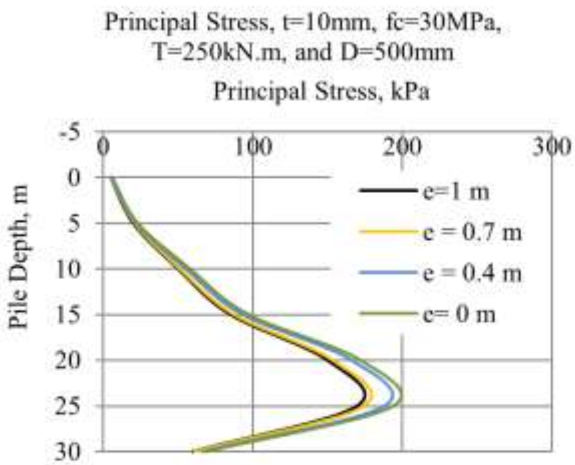

Figure 7. c: Principal stress along pile when change load eccentricity.

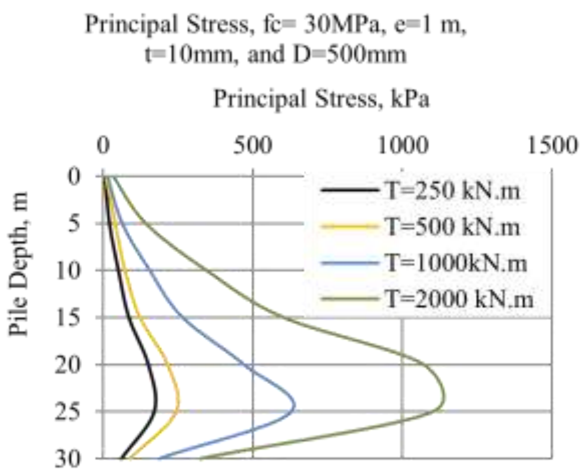

Figure 7. d: Principal stress along pile when change torsion load.

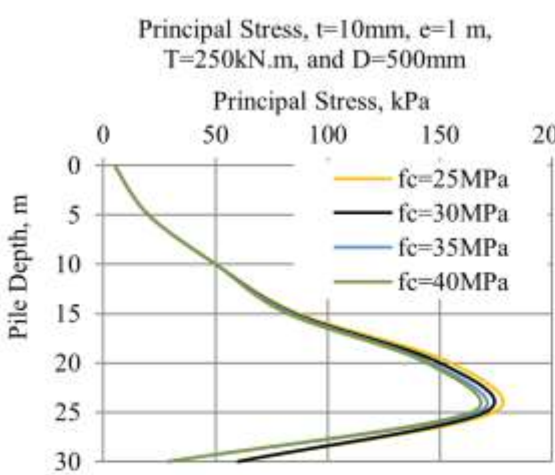

Figure 7. e: Principal stress along pile when change concrete compressive strength.

3. 7 Von miss stress

Von Mises stress is used to predict the yield strength of materials under load. The same procedure, which was described in the previous section dealing with pile displacement, was also adopted in this study to evaluate pile Von Mises stress. Figures (8-a), (8-b), (8-c), (8-d) and (8-e) illustrate the noticeable variation in von miss stress along the pile depth, considering pile diameter, steel tubular wall thickness, load eccentricity, torque magnitude, and concrete compressive strength. Figure (8-a) illustrates the alteration in Von Mises stress with depth for various pile diameter. It is evident from the figure, with an increase in pile diameter, Von Mises stress decreases, owing to the increase in diameter leading to a higher moment of inertia. This results in higher resistance to the applied load. Therefore, the stress distribution along the pile depth is reduced compared to pile with a smaller diameter. Von Miss stress was found to be similar regardless of the variation in pile diameter. Based on Figures (8-b) and (8-d), it was observed that the maximum values of Von Mises stress occurred when the parameters were greatest value of steel tubular wall thickness, and torque magnitude respectively, while the minimum values of Von Mises stress were observed when those parameters were at their lowest values of steel tubular wall thickness, and torque magnitude respectively. Many variable were found to influence the variation of Von Mises stress, including pile cross-section, pile moment of inertia, pile resistance to applied load, pile stiffness, load transfer to soil, and soil resistance. Figures (8-b) and (8-d) showed identical behavior regardless of the variation in wall thickness and torque value. Figure (8-c) illustrates the alteration in Von Mises stress with depth for various load eccentricities. The maximum Von Mises stress was observed when there was no load eccentricity, while the minimum stress occurred at e=1m. This variation was attributed to the drop in pile resistance to the applied load. Figure (8-e) illustrates the alteration in Von Mises stress with depth for various of concrete compressive strength. It is clear from the figure that compressive strength has a minor effect on the stress distribution along the pile depth. Therefore, all curves appears identical in behavior regardless of the compressive strength values.

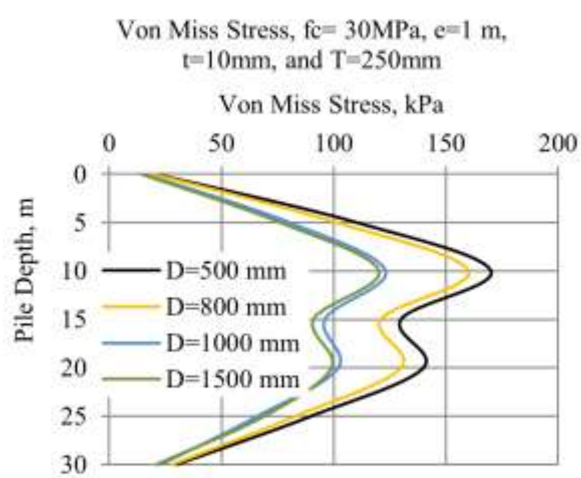

Figure 8. a: Von miss stress along pile when change pile diameter.

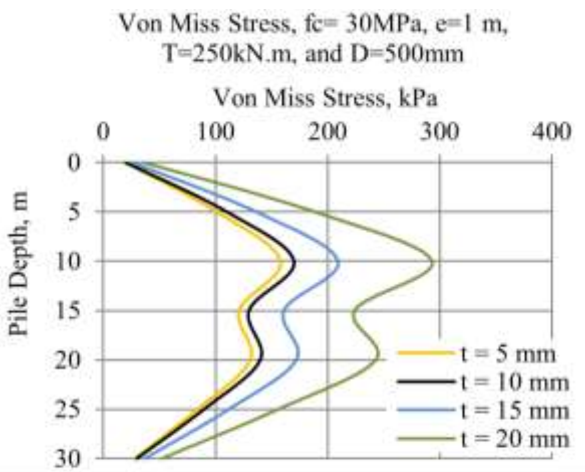

Figure 8. b: Von miss stress along pile when change pile thickness.

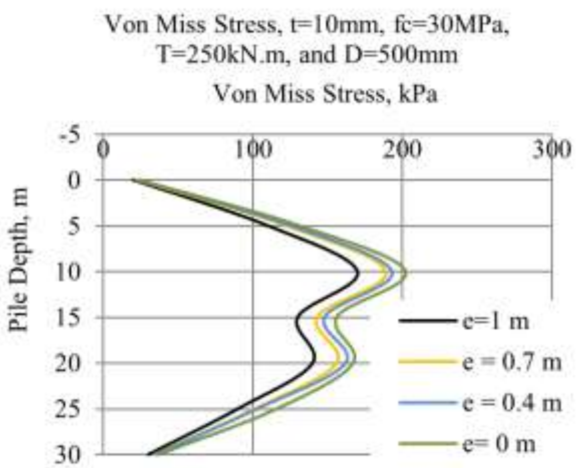

Figure 8. c: Von miss stress along pile when change load eccentricity.

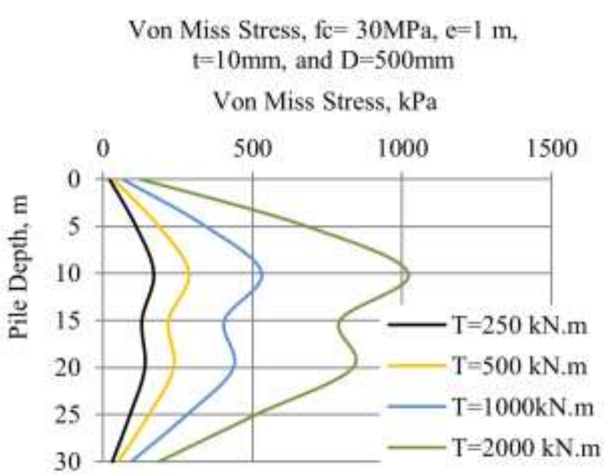

Figure 8. d: Von miss stress along pile when change torsion load.

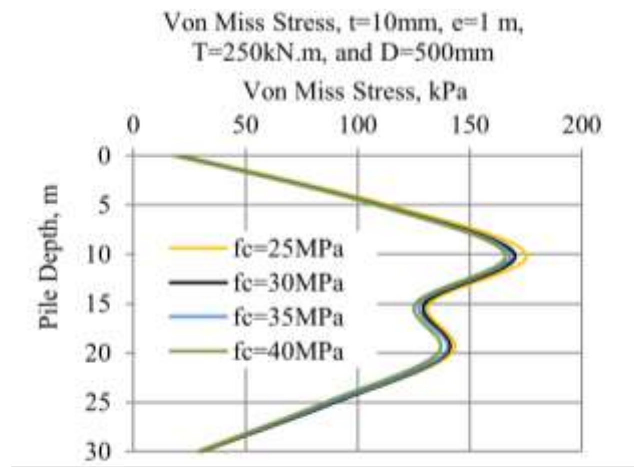

Figure 8. e: Von miss stress along pile when concrete compressive strength.

3. 8 Soil reaction

The same procedure, which was described in the previous section dealing with pile displacement, was also adopted in this section to investigate soil reaction. Figures (9-a), (9-b), (9-c), (9-d), and (9-e) illustrate the noticeable variation in soil reaction along the pile depth, considering pile diameter, steel tubular wall thickness, load eccentricity, torque magnitude, and concrete compressive strength. Figure (9-a) shows the variation in soil reaction along the pile when various pile diameter were adopted. It was shown that with an increase in pile diameter, the soil reaction gradually decreased. This behavior was attributed to the fact that an increase in pile diameter reduces the load transferred to the soil. In adiition, the response of soil was reduced due to the lower load transfer between the pile and the surrounding soil. Figure (9-b) shows the variation in soil reaction along the pile when various steel tubular wall thickness were considered. It was observed from the figure that with an increase in wall thickness, the soil reaction also increased, owing to the fact that the pile diameter was considered small, so the load transfer from pile to the soil was increased. Additionally, the soil reaction became large due to the increased load transfer from the pile to the surrounding soil. Figure (9-c) shows the variation in soil reaction along the pile with different load eccentricities. From the figure, the maximum soil reaction occurred when the load eccentricity was equal to zero (no load eccentricity), while the minimum soil reaction was recorded when the load eccentricity was equal to 1 m above the ground level. The variation in soil reaction results depended mainly on pile stiffness, soil stiffness, pile diameter, and load transferred to the soil. Figure (9-d) shows the variation in soil reaction along the pile when variouse torque magnitudes were applied. It was evident from the figure with an increase in torque magnitude, the soil reaction increased, owing to the increase in load transfer to the soil, which was directly reflected directly in the soil reaction. . Figure (9-e) shows the variation in soil reaction along the pile when variouse concrete compressive strengths were adopted. It can be inferred from the figures that the compressive strength had a minor effect on the soil reaction distribution along the pile, regardless the values of concrete compressive strength.

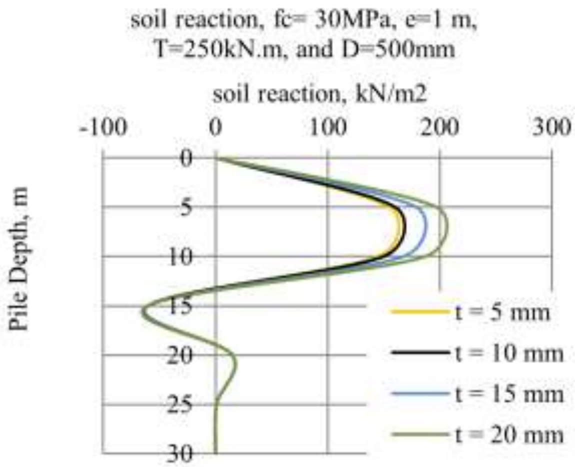

Figure 9. a: Soil reaction along pile when change pile diameter.

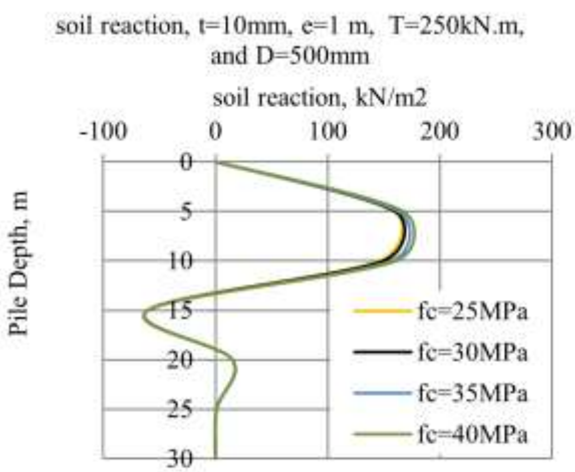

Figure 9. b: Soil reaction along pile when change pile thickness.

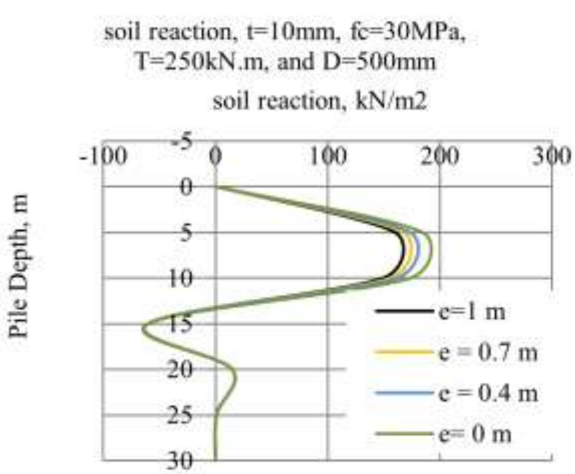

Figure 9. c: Soil reaction along pile when change load eccentricity.

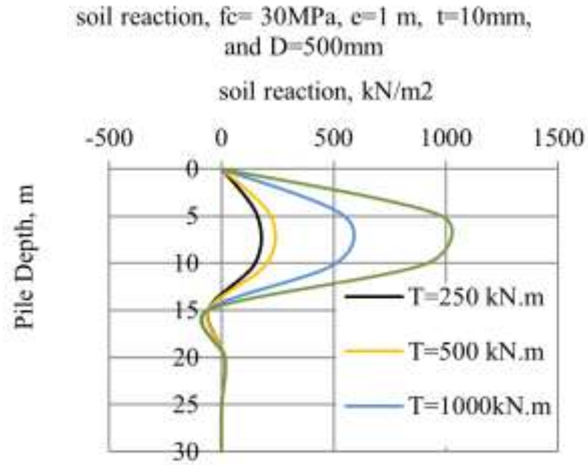

Figure 9. d: Soil reaction along pile when change torsion load.

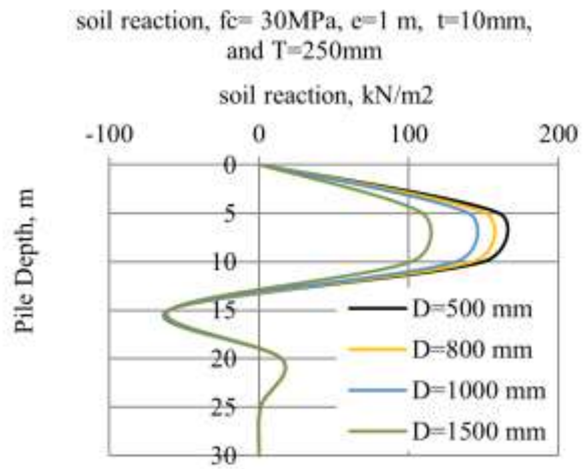

Figure 9. e: Soil reaction along pile when change concrete compressive strength.

Conclusion

Pile foundations have been widely used to support supperstructure, therefore, it is considered essential to study the behavior of these structural elements under different loading conditions. From this paper, the following conclusions can be inferred: pile diameter or pile moment of inertia, steel tubular wall thickness, soil properties, concrete compressive strength, load eccentricity, and torque magnitude are identified as important variables that should be investigated clearly to avoid any potential failure that may occure in pile during the serviceability life of the pile. It has been inferred from the study that pile diameter, pile wall thickness, load eccentricity, and torque magnitude are considered major variables that must be adopted into pile design under harmonic dynamic loading, while concrete compressive strength is regarded as a minor variable. The variation in pile response is found to relies on pile stiffness, soil stiffness, and load transfer from pile to soil. From analysis, it was shown that an increase in pile diameter resulted in a displacement reduction of 24%, with an increase in steel wall thickness led to a reduction in displacement by 19 %, and an increase in torsional load caused the displacement to rise by 27 %.

For any case, the shear force profile was observed to change from positive to negative at a distance between (5-10) m, or approximately 7.5m measured from the pile head. Similarly, the bending moment profile was found to change from positive to negative at a distance between (10-15) m measured from the pile head. After 15m from the pile head, below the ground surface, the torsional effect may be considered negligible, because the torsional behavior profile remains constant without any noticeable change. The skin friction profile was found to shift from negative to positive at a depth of 10m from the pile head, below the ground surface regardless of the case study. The pile was observed to behave nonlinearly in the distribution of principal stress and von Miss stress along the pile depth respectively. The soil reaction behavior is described as complex and nonlinear.

References

[1] Wang, Z., Jiang, J., Wang, S., Fu, C. and Yang, D. Analysis on bearing behavior of single pile under combined action of vertical load and torque in expansive soil. *Applied Sciences*, **13**(7), 4133, doi: 10.3390/app13074133, (2023).

[2] Hasan, A.Q. and Qasim, R.M. Investigating the response of single pile under pure torsion. *J. Appl. Eng. Sci* **12**, 37-42, doi: 10.2478/jaes-2022-0006, (2023).

[3] Ma, W., Shan, Y., Xiang, K., Wang, B. and Zhou, S. Torsional dynamic response of a pipe pile in homogeneous unsaturated soils. *Computers and Geotechnics* **143**, 104607, doi: 10.1016/j.compgeo.2021.104607, (2022).

[4] Wang, B., Zhu, M., Gong, W. and Cao, G. Variational Elastic Solution for an End Bearing Pile Subjected to Dynamic Torsional Loading. *Soil Mechanics and Foundation Engineering* ***59***(2), 126-133, doi: 10.1007/s11204-022-09792, (2022).

[5] Wang, S.W., Jiang, J., Fu, C.Z., Ou, X.D. and Tang, J. Analysis of the bearing characteristics of single piles under vertical and torsional combined loads. *Advances in Civil Engineering* ***2021***(1), 8896673, doi: 10.1155/2021/8896673, (2021).

[6] Li, X., Zhang, Z. and Sheng, J. Exact solution for the torsional vibration of an elastic pile in a radially inhomogeneous saturated soil. *Journal of Mathematics* ***2021***(1), 6644057, doi: 10.1155/2021/6644057. (2021).

[7] Le, Y., Wang, N., Hu, W., Geng, D. and Jiang, Y. Torsional dynamic impedance of a stepped pile based on the wedged soil model. *Computers and Geotechnics* **128**, 103854, doi: 10.1016/j.compgeo.2020.103854, (2020).

[8] Hasan, A., Q., Qasim, R., M., Effects of soil domain size on torsional response of offshore platform. *International transaction journal of engineering, management, & applied sciences & technologies,* **11** (9), doi: 10.14456/ITJEMAST.2020.166

[9] Nimbalkar, S.S., Punetha, P., Basack, S. and Mirzababaei, M. Piles subjected to torsional cyclic load: numerical analysis. *Frontiers in Built Environment* **5**, 24, doi.org/10.3389/fbuil.2019.00024, (2019).

[10] Li, Z., Gao, Y. and Wang, K. Torsional vibration of an end bearing pile embedded in radially inhomogeneous saturated soil. *Computers and Geotechnics* **108**, 117-130, doi: 10.1016/j.compgeo.2018.12.014, (2019).

[11] Zheng, C., Liu, H., Ding, X. and Lv, Y. Torsional dynamic response of a large-diameter pipe pile in viscoelastic saturated soil. *International Journal for Numerical and Analytical Methods in Geomechanics* **38**(16), 1724-1743, doi: 10.1002/ nag.2279, (2014).

[12] Basack, S., Sen, S. and Dey, S. An analytical solution for single pile subjected to torsion. In *Proceedings of Indian geotechnical conference December,* 15-17, (2011).

[13] Wang, K., Zhang, Z., Leo, C.J. and Xie, K. Dynamic torsional response of an end bearing pile in transversely isotropic saturated soil. *Journal of Sound and Vibration* **327**(3-5), 440-453, doi: 10.1016/j.jsv.2009.06.017, (2009).

[14] Wang, K., Zhang, Z., Leo, C.J. and Xie, K. Dynamic torsional response of an end bearing pile in saturated poroelastic medium. *Computers and Geotechnics* **35**(3), 450-458, doi:10.1016/j.compgeo.2007.06.013, (2008).

[15] Chen, G., Cai, Y., Liu, F. and Sun, H. Dynamic response of a pile in a transversely isotropic saturated soil to transient torsional loading. *Computers and Geotechnics* **35**(2), 165-172, doi: 10.1016/j.compgeo.2007.05.009, (2008).

[16] Wang, G., Ge, W., Pan, X. and Wang, Z. Torsional vibrations of single piles embedded in saturated medium. *Computers and Geotechnics* **35**(1), 11-21, doi:10.1016/j.compgeo.2007.02.001, (2008).

[17] Cai, Y., Chen, G., Xu, C. and Wu, D. Torsional response of pile embedded in a poroelastic medium. *Soil Dynamics and Earthquake Engineering* **26**(12), 1143-1148, doi: 10.1016/j.soildyn.2005.10.009, (2006).

[18] Chen, L. and Wang, G. Torsional vibrations of elastic foundation on saturated media. *Soil Dynamics and Earthquake Engineering* **22**(3), 223-227, (2002).

[19] Militano, G. and Rajapakse, R.K.N.D. Dynamic response of a pile in a multi-layered soil to transient torsional and axial loading. *Geotechnique* **49**(1), 91-109, (1999).

[20] Novak, M. and Howell, J.F. Torsional vibration of pile foundations. *Journal of the Geotechnical Engineering Division* **103**(4), 271-285, (1977).

[21] Rasheed, M.M. THE EFFECT OF SIFCON ON TORSIONAL BEHAVIOR OF REINFORCED CONCRETE BEAMS. *Journal of Engineering and Sustainable Development* **26**(4), 52-62, doi: 10.31272/jeasd.26.4.6, (2022).

[22] Bajad, M. and Patil, R.D. SEISMIC ANALYSIS OF MULTISTORIED OPEN GROUND STORY BUILDING WITH DIAGONAL STRUT AND SHEAR WALLS. *Journal of Engineering and Sustainable Development* **28**(02), 160-177, (2024).

[23] Mnati, A.A. and Resan, K.K. Production of ductile cast iron by recycling gray cast iron scrap with adding various local materials. *Journal of Engineering and Sustainable Development* **27**(1), 117-126, doi: 10.31272/jeasd.27.1.10 (2023).

[24] A., al-Mubarak, Abdulameer, R.M., Qasim, Rafi Mohammed, A., Al-Yousuf, Ayad, Numerical evaluation of load transfer between adjacent piles under varying load conditions,. *International Journal of Advanced Technology and Engineering Exploration*, (2025).

[25] Al Amli, A.S., Al-Ansari, N. and Laue, J., Behavior of reinforcement bars in foundation with soil to satisfy

sustainability. *Journal of Engineering and Sustainable Development* **27**(5), 558-564, doi: 10.31272/jeasd.27.5.1 (2023).

[26] Hasan, A.Q. and Younus, Y.M. Used Isolation System to Reduce the Response of Offshore Structure Considering Soil Structure Interaction. *Civil And Environmental Engineering Reports* **19**(2), 662-675, doi: 10.2478/cee-2023-0060, (2023).

[27] Al-Defae, A.H., Caucis, K. and Knappett, J.A. Aftershocks and the whole-life seismic performance of granular slopes. *Géotechnique* **63**(14), 1230-1244, doi: 10.1680/geot.12.P.149, (2013).

[28] Hasan, A.Q. Optimal shape of concrete tanks under seismic load considering soil-structure interaction., *Al Qadisiyah Journal for Engineering Sciences* **18**(1), 65–71, (2025).